Erythrocyte microparticles can induce kidney vaso-occlusions in a murine model of sickle cell disease

Stéphane M. Camus,[1] Blandine Gausserès,[1] Philippe Bonnin,[2] Laurent Loufrani,[3] Linda Grimaud,[3] Dominique Charue,[1] Joao A. De Moraes,[1] Jean-Marie Renard,[1] Alain Tedgui,[1] Chantal M. Boulanger,[1] Pierre-Louis Tharaux,[1] and Olivier P. Blanc-Brude[1]

[1]Paris Center for Cardiovascular Research, Inserm Unité Mixte de Recherche (UMR)s-970, Hôpital Européen Georges Pompidou, et Université Paris Descartes, Sorbonne Paris Cité, Paris, France; [2]Université Paris Diderot, Sorbonne Paris Cité, Inserm, UMRs-965, Assistance Publique des Hopitaux de Paris, Hôpital Lariboisière, Physiologie Clinique-Explorations-Fonctionnelles, Paris, France; [3]Centre National de Recherche Scientifique UMRs-6214 et Inserm U1083, CHU Angers, Université d'Angers, Angers, France

Patients with sickle cell disease suffer from painful crises associated with disseminated vaso-occlusions, increased circulating erythrocyte microparticles (MPs), and thrombospondin-1 (TSP1). MPs are submicron membrane vesicles shed by compromised or activated cells. We hypothesized that TSP1 mediates MP shedding and participates in vaso-occlusions. We injected TSP1 to transgenic SAD mice with sickle cell disease and characterized circulating phosphatidylserine+ MPs by FACS. TSP1 stimulated MPs in plasma and initiated vaso-occlusions within minutes. In vitro, TSP1 triggered rapid erythrocyte conversion into spicule-covered echinocytes, followed by MP shedding. MP shedding was recapitulated by peptides derived from the TSP1 carboxyterminus. We purified MPs shed by erythrocytes in vitro and administered them back to SAD mice. MPs triggered immediate renal vaso-occlusions. In vitro, MPs triggered the production of radical oxygen species by endothelial monolayers, favored erythrocyte adhesion, and induced endothelial apoptosis. MPs also compromised vasodilation in perfused microvessels. These effects were inhibited by saturating MP phosphatidylserine with annexin-V, or with inhibitors of endothelial ROS production. We conclude that TSP1 triggers erythrocyte MP shedding. These MPs induce endothelial injury and facilitate acute vaso-occlusive events in transgenic SAD mice. This work supports a novel concept that toxic erythrocyte MPs may connect sickle cell anemia to vascular disease. (*Blood*. 2012;120(25): 5050-5058)

Introduction

Sickle cell disease (SCD) is a form of hemolytic anemia that results from a point mutation (HbS) in the gene of the globin β-chain. The mutation makes HbS susceptible to polymerize during hypoxic stress, producing long intracellular fibers that are responsible for drastic membrane and cytoskeletal remodeling. The HbS fibers polymerize and depolymerize in response to blood oxygenation and deoxygenation cycles. The repeated changes in red blood cell (RBC) shape cause a permanent loss of the biconcave phenotype, producing condensed cells with diverse degrees of crenation, and covered in cone-shaped membrane figures known as spicules.[1-3] The remodeled erythrocytes become progressively dehydrated and rigid. Fully and irreversibly remodeled erythrocytes are termed sickle erythrocytes with respect to their ultimate shape.

Sickle erythrocytes display a strong predisposition to adhere to the endothelium, get trapped in small capillaries and reduce blood flow. Highly vascularized organs, such as kidneys, bones, and lungs are the seat of disseminated vascular occlusions and recurrent ischemic injury.[4] In some of these organs, ischemia causes extremely painful episodes termed vaso-occlusive crises (VOCs). These crises are attributed to stress factors, such as hypoxia, physical exercise, infection, trauma, or stress. However, the molecular basis for the development of vaso-occlusions in SCD has yet to be explained and several different triggers of VOCs may exist.

After getting trapped in capillaries, rigid sickle erythrocytes are thought to break apart in a process generally termed intravascular hemolysis, resulting in anemia. VOCs and hemolysis are associated with the release of submicron erythrocyte membrane vesicles called microparticles (MPs) into the bloodstream.[1] Steady-state SCD patients display circulating levels of MPs that are 3- to 10-fold higher than those of healthy subjects, as revealed by the detection of phosphatidylserine-positive (PS^+) MPs.[5-8] Circulating MP levels in SCD patients may also increase 0.3- to 3-fold during VOCs versus steady-state.[9-11] In steady-state SCD, MPs are mostly of erythrocyte origin, but they can also originate from platelets,[5] endothelial cells, and leukocytes during VOCs.[6,8,9,11] Erythrocyte MPs are generally assumed to be a consequence of intravascular erythrocyte vesiculation in SCD, in possible connection with hemolysis, but the precise molecular regulation of intravascular hemolysis and MP shedding remains unknown. On the other hand, the impact of circulating erythrocyte MPs on the physiopathology of SCD is unclear. Fundamental studies have suggested that circulating MPs may enhance erythrocyte aggregation[5] and possibly favor blood coagulation.[11]

Submitted February 22, 2012; accepted August 29, 2012. Prepublished online as *Blood* First Edition paper, September 13, 2012; DOI 10.1182/blood-2012-02-413138.

The online version of this article contains a data supplement.

The publication costs of this article were defrayed in part by page charge payment. Therefore, and solely to indicate this fact, this article is hereby marked "advertisement" in accordance with 18 USC section 1734.

SCD patients also display abnormal platelet biology with elevated circulating levels of the major platelet protein thrombospondin-1 (TSP1). TSP1 increases sharply during VOCs (+80% average; up to +400%).[12] Indeed, SCD platelets show dilated, open canalicular systems and empty secretory α-granules,[5,13] coherent with chronic platelet activation, particularly during VOCs. TSP1 is a large trimeric protein stored in platelet α-granules, that accounts for 25% of proteins secreted during thrombosis, when it generates steep and local gradients.[14,15] TSP1 can also be secreted by vascular cells challenged with thrombin,[16] hypoxia,[17,18] mechanical injury,[19] or abnormal blood flow.[20-22] TSP1 has been found to trigger SCD erythrocyte adhesion in vitro.[23-26] Moreover, activated platelet supernatant induces strong adhesion of sickle erythrocytes to cultured vascular endothelium.[23]

In this report, we postulated that TSP1 facilitates vaso-occlusive events and participate in intravascular erythrocyte vesiculation. We investigated the links between TSP1, vascular occlusions and the formation of circulating erythrocyte MPs in transgenic SAD mice, an experimental model of SCD.[27] We also aimed to clarify the role of circulating erythrocyte MPs in the formation of vascular occlusions.

Methods

For more information on materials and methods, see supplemental Methods (available on the *Blood* Web site; see the Supplemental Materials link at the top of the online article).

Materials

Human recombinant TSP1 was produced by EMP-Genetech. Synthetic peptides[28] 4N1-1 (RFYVVMWK) and 4N1-2 (RFYVVM) were obtained from Bachem, and 4NGG (RFYGGMWK) is manufactured by Genecust. Di-aminidophenylindol (DAPI), RNase A and propidium iodide were from Sigma-Aldrich.

Murine model of sickle cell disease

We used 10- to 14-week-old SAD transgenic male mice on C57bl6J background obtained from Dr Beuzard[27] and carrying the human *βS β^{6}Val*, *βS-Antilles β^{23}Ile*, and *D-Punjab β^{121}Glu globin β-chain* transgene. All procedures for study animal care and euthanasia followed the European Community standards (authorization No. 00577) and were validated by the local Inserm ethics committee.

Kidney vaso-occlusions in mice

We characterized renal vaso-occlusions in SAD transgenic mice according to our previously published method,[29,30] in response to the intravenous administration of TSP1 or purified erythrocyte MPs. Briefly, anesthetized and shaved mice were placed on a heating blanket (38°C). A pulsed Doppler spectrum was recorded with a Vivid 7 echograph (GE Medical Systems) equipped with a 12-MHz linear transducer (12L). Data were transferred to an EchoPAC ultrasound image analysis workstation (GE Medical Systems). Peak systolic, end-diastolic and time-average mean blood flow velocity were measured. Cardiac output was calculated with the following formula:

$$CO = [(V^{mean} \times 60) \times (\pi \times (Dpa/2)^2)],$$

(CO = cardiac output in mL/min, V^{mean} = mean time-averaged blood flow velocity in cm/s, Dpa = pulmonary artery diameter in cm; n = 5 to 8 measurements). Kidney sections were stained by Masson trichrome to assess vascular congestion by phase-contrast microscopy, as erythrocyte aggregates occluding kidney vessels. TSP1 (1 mg/kg) was injected. After 5 minutes, whole blood was collected, centrifuged (400*g*, 15 minutes), and double centrifuged (12 500*g*, 5 minutes) to eliminate cells and generate platelet-free plasma (PFP) with minimal platelet activation. Blood flow velocity was also measured in the basilar artery, and careful monitoring of pain was performed between MP injection and euthanasia.

Erythrocyte preparations

To purify erythrocytes, mouse blood was obtained through retro-orbital sinus puncture, mixed with anticoagulant heparin buffer (5 UI/mL), and collected on citrated tubes. Blood was centrifuged on Histopaque-1083 (Sigma-Aldrich) density gradients (600*g*, 25 minutes). Erythrocyte surface CD47 expression was assessed by FACS. Fresh erythrocytes were immunoreacted with mouse-specific anti-CD47 monoclonal antibody (clone mIAP301; BD Bioscience), or matched irrelevant isotype. Erythrocyte phenotypes were analyzed by scanning electronic microscopy. Briefly, mouse erythrocytes were fixed and embedded in Epon epoxy resin. Contrasted sections were examined with a JEOL JEM 1010 microscope. Average apparent spicule number was determined by direct counting. Crenation and sickle cell formation were confirmed by phase contrast microscopy.

MP characterization

Erythrocytes were suspended in polyvinylpyrrolidone (31 mPa/s) and placed in a rotating type LORCA ektacytometer (R&R Mechatronics), in the absence or presence of TSP1 (25 μg/mL), or TSP1-derived peptides 4N1-1 or 4N1-2 (25μM). Shear rate was applied (1500 seconds^{-1}; 2.5 minutes). Supernatant PS^+ MPs were labeled with FITC-conjugated annexin-V (Roche Diagnostics) diluted in reaction buffer with 5mM $CaCl_2$ and quantified as previously described[31] on an EPICS XL flow cytometer (Beckman Coulter). MPs were identified in forward light scatter (FSc) and side-angle light scatter (SSc) as events of 0.1 to 1 μm in diameter. MP-size events were analyzed with respect to calibrated fluorescent microbeads (Flowcount). To determine erythrocyte origin, MPs were double-labeled with rat mouse-specific anti-Ter119 antibody (Biolegend via Ozyme), or matched irrelevant isotype.

Endothelial cell culture

SV40-transformed mouse lymph node endothelial cells (SVEC4-10; ATCC) were grown to confluence and incubated with 25 MPs/μL for up to 2 hours. 5-(6-)carboxy-2′,7′-difluorodihydrofluorescein diacetate (H_2DFF-DA; 10μM) was then added to determine ROS production. Fluorescence was read in an automated plate reader. For adhesion experiments, MP-primed SVEC monolayers were washed and incubated with RBC suspensions (1.10^6 RBC/mL). After 30 minutes, adherent erythrocytes were counted by phase contrast microscopy in 5 random fields per well (400×), n = 3 to 6 in triplicates. For cell cycle analysis, SVEC were cultured up to 70% confluence and placed in DMEM with 0.05% NCS with or without RBC MPs. After 36 hours, SVEC were fixed and incubated in 0.05% Triton X100, 100 μg/mL RNase A, 50 μg/mL propidium iodide. DNA profiles were collected by FACS and divided as sub-G_1 (apoptosis), G_0/G_1 (rest) and G_2/M (proliferation) phases. Data shown as mean percentage of cells, n = 3.

Microvascular dilation

Mouse mesenteric arterial segments were canulated and mounted in a video-monitored perfusion system as described.[32] Arterial segments were bathed in physiologic salt solution (PSS) maintained at pH 7.4, with pO_2 and pCO_2 of 160 mmHg and 37 mmHg, respectively. Arterial diameter was continuously recorded by video (Living System Instrumentation) with intraluminal pressure was set at 75 mmHg, using a Biopac MP 100 acquisition system and Acknowledge Version 3.7.3 software (Biopac). Arterial segments were preconstricted with phenylephrine (PE). ACH (10^{-7}-10^{-4}M) was then gradually applied. Sodium nitroprusside (SNP, 100μM) was tested after ACH. After de novo PE-induced preconstriction, MPs were then perfused through the segments and ACH was applied again. SNP (100μM) was then tested. Finally, passive diameter was determined with Ca^{2+}-free PSS containing

ethylenebis-(oxyethylenenitrolo) tetra-acetic acid (2mM), SNP (10μM), and papaverine (10μM).

Statistical analysis

For in vivo vaso-occlusions and ex vivo vasodilation experiments, intergroup comparisons (5-6 animals/group) were performed by variance analysis (1- or 2-way ANOVA), completed by posthoc Bonferroni test, or/and Student *t* test (MedCalc Version 9.3 software). In vitro experiments were repeated at least 3 times and statistical analysis was performed with paired or unpaired Student *t* tests as appropriate. Results were expressed as mean ± SEM. Statistical significance was achieved when P value $< .05$.

Results

Plasma TSP1 and kidney vaso-occlusions in SAD mice

In SAD mice, raising plasma TSP1 by intravenous injection (1 mg/Kg) induced a rapid 20% reduction in the mean blood flow velocity in right renal arteries, progressing to 35% after 5 minutes (Figure 1A; $P < .05$ vs control), as shown in representative echo-Doppler waveforms (Figure 1B). In SAD mice, systolic blood flow velocity was unchanged after TSP1 injection, but diastolic and mean blood flow velocities were dramatically decreased. TSP1 did not affect cardiac output (Figure 1C) or heart rate (Figure 1D). Histologic assessment by Masson trichrome staining revealed red blood cells aggregates and renal capillary congestion in the medula (Figure 1E). TSP1 did not modify kidney blood flow velocities, cardiac parameters, or histology in wild-type mice.

TSP1 enhanced erythrocyte vesiculation

We collected platelet-free plasma (PFP) after TSP1 injection to mice and quantified circulating PS^+ MPs (Figure 2A). At rest, SAD PFP contained twice as many MPs than wild-type PFP (880 vs 400 MPs/μL, respectively; $P < .05$). TSP1 injections triggered a 3-fold rise in plasma PS^+ MPs within 5 minutes in both wild-type and SAD mice ($P < .05$ for treated vs control SAD, or vs treated wild-type mice). Moreover, we found that Ter119+ erythrocyte MPs jump from 3% to 20% PS+ MPs in WT mice injected with TSP1, whereas Ter119+ erythrocyte MPs increase from 18% to 26% in SAD mice ($P < .05$ vs basal levels; supplemental Figure 1).

In erythrocytes and reticulocytes, highly conserved VVM sequences in the TSP1 carboxyterminus are thought to modulate the activation of CD47,[33-36] also known as integrin-associated protein (IAP) in platelets and leukocytes, a key constituent of the Rhesus protein complex. CD47 activation enhances integrin avidity and mediate the pro-adhesive effects of TSP1 on sickle erythrocytes.[23-26] Synthetic carboxyterminal peptides including 4N1-1[28] reproduce some functions of TSP1. The peptides may also have additional effects.[33-36] Injecting peptide 4N1-1 to mice induced a 3-fold rise in circulating PS^+ MPs ($P < .05$ vs control mice), similar to TSP1 injection. FACS experiments showed that the majority of wild-type and SAD erythrocytes expressed cell-surface CD47 (85%; Figure 2B).

TSP1 induced phenotypic modifications in erythrocytes

We asked whether TSP1 could directly modify the phenotype and vesiculation of fresh purified erythrocytes in vitro. We placed erythrocytes in a Lorca ektacytometer, in dynamic conditions matching arteriolar shear rates.

Scanning electron microscopy confirmed that fresh wild-type erythrocytes are nearly all biconcave discocytes (> 95%; Figure 2C), which was confirmed by phase-contrast microscopy (100×).

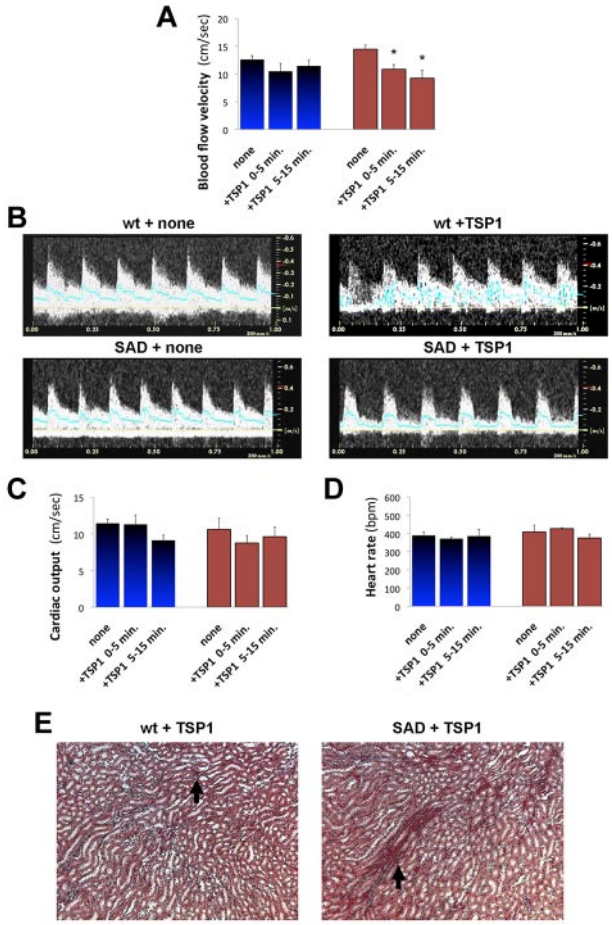

Figure 1. TSP1 triggers vaso-occlusive crises in SAD mice. We injected recombinant TSP1 (1 mg/kg) intravenously to wild-type (WT; blue) and SAD transgenic mice (brown) and characterized vaso-occlusions in kidneys by echo-Doppler recording of hemodynamic parameters. (A) We determined mean blood flow velocity (cm/s) in the right renal artery, before (none), or within 1 to 5 minutes, or between 5 and 20 minutes of TSP1 injection (*$P < .05$ vs control, none). (B) Representative echo-Doppler waveforms in the renal artery of WT and SAD mice before and after injection of TSP1. We also determined the heart rate (C; beats per minutes) and calculated the cardiac output (D; mL/min) from recording in the pulmonary artery. (E) Histologic analysis of wild-type and SAD kidneys 5 minutes after TSP1 injection by Masson trichrome. Black arrows show areas of vascular congestion and erythrocyte deposits.

TSP1 induced rapid erythrocyte crenation and the formation of cone-shaped membrane spicules by more than 10-fold, up to 10% ($P < .05$ vs control). In resting SAD erythrocytes, only 5% cells were typical elongated sickle cells, but 30% displayed a variety of shapes with elongated, crenated, and spicule-covered bodies (Figure 2C). Addition of TSP1 further increased the proportion of SAD echinocytes carrying a highly heterogeneous number of long and thin spicules, reaching 50% ($P < .05$ vs control; Figure 2C image). TSP1 increased the proportion of spicule-covered echinocytes, but did not affect the proportion of sickle-shaped cells. Concurrently, TSP1 induced a doubling in PS+ MP shedding in SAD cells ($P < .05$ vs SAD or wt controls; Figure 2D). This effect of TSP1 was significant above 10 μg/mL (supplemental Figure 1).

Next, we evaluated the effects of TSP1 carboxyterminal peptide 4N1-1, truncated control 4N1-2 and mutated control 4NGG (no VVM motif). Scanning electron microscopy revealed that 4N1-1 triggered phenotypic changes like TSP1 (Figure 2E-F), with a drastic 10-fold increase in wild-type echinocytes and a 50% increase in SAD echinocytes ($P < .05$; Figure 2F). Elongated

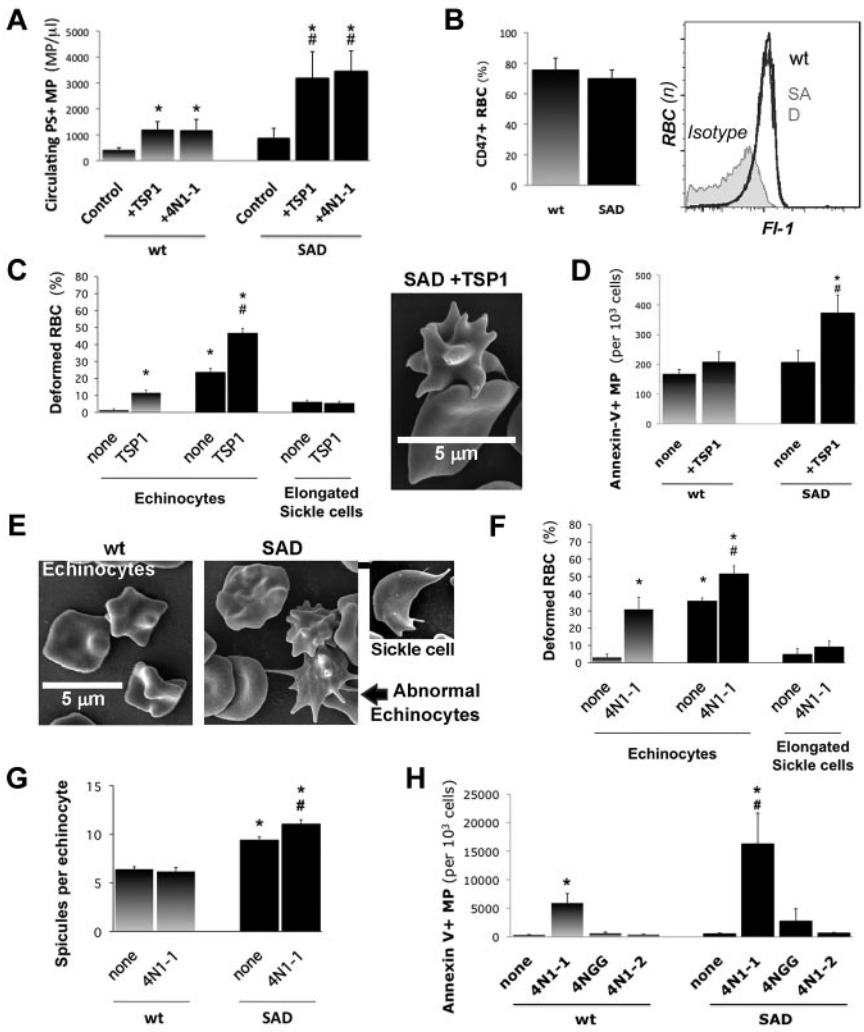

Figure 2. TSP1 triggers MP shedding via CD47. (A) We injected recombinant TSP1 intravenously to wild-type (WT) and SAD mice (1 mg/kg). Within 10 minutes, we collected platelet-free plasma to quantify circulating PS$^+$ MPs by FACS after annexin-V labeling (*$P < .05$ vs controls, #$P < .05$ vs wild-type +TSP1. (B) We determined the surface expression of CD47 on WT and SAD RBC by FACS, expressed in percent (left). Plot of CD47-labeling in Fl-1 (right). (C-D) SAD and WT RBCs were placed in polyvinylpyrrolidone. Shear rate was applied with an ektacytometer (1500 seconds^{-1}; 2.5 minutes) with or without addition of TSP1 (20 μg/mL). RBCs were prepared for scanning electron microscopy. (C) Biconcave discocytes, spicule-covered echinocytes, and elongated sickle cells were quantified by phase-contrast microscopy (SAD in solid bars; *$P < .05$ vs WT controls, none; #$P < .05$ vs SAD control, none). (D) Supernatant PS$^+$ MPs were quantified by FACS after annexin-V labeling (*$P < .05$ vs SAD controls; #$P < .05$ vs wt+TSP1). In other experiments, WT and SAD RBCs were treated with 4N1-1, or control peptides 4N1-2 and 4NGG (10μM; 10 minutes) in RPMI-1640. (E) SAD and WT erythrocytes treated with 4N1-1. (F) Biconcave discocytes, spicule-covered echinocytes, and elongated sickle cells were quantified (SAD in solid bars; *$P < .05$ vs WT controls, none; #$P < .05$ vs WT+TSP1 control, none). (G) Spicules on WT and SAD echinocytes were counted (*$P < .05$ vs control wild-type RBC, none; #$P < .05$ vs SAD controls). (H) Supernatant PS$^+$ MPs were quantified by FACS after annexin-V labeling (*$P < .05$ vs controls, none; #$P < .05$ vs WT+TSP1).

sickle cells remained unaffected. SAD echinocytes showed an abnormal multiplication of thin, long and apparently fragile spicules (+15%; $P < .05$ vs SAD and WT controls). Spicule numbers and dimensions remained homogenous in wild-type cells (Figure 2G). Concurrently, 4N1-1 triggered a 40-fold rise in SAD erythrocyte MP shedding and a 30-fold increase in wild-type erythrocytes ($P < .05$ vs control 4N1-2). 4N1-2 and 4NGG had no effect. SAD erythrocytes shed more MPs than healthy erythrocytes ($P < .05$ vs wild-type; Figure 2D-H).

Erythrocyte MPs and kidney vaso-occlusions in SAD mice

To investigate the impact of erythrocyte MPs on vascular occlusions in SAD mice, we administered purified erythrocyte MPs intravenously, at concentrations selected on the basis of our measurements in WT and SAD mice and those reported in humans (400 MPs/μL in health and 3- to 10-fold higher in steady state SCD[5,7,8]). PS$^+$ MP levels in SCD patients increase up to 3-fold during VOCs[9-11] and these MPs are predominantly of erythrocyte origin (20%-75%), whereas erythrocyte MPs represent less than 5% of circulating MPs in health.[6,8,9,11] Erythrocyte MPs were injected into mice at 8×10^3 MPs/mouse to induce a 20% increase in circulating erythrocyte MPs (supplemental Methods). In other experiments, we injected 300×10^3 MPs/mouse to increase total circulating PS+ MP levels by one-third compared with wild-type mice.

At 8×10^3 MPs/mouse, wild-type erythrocyte MPs had no significant impact on blood flow velocity in wild-type renal arteries (Figure 3A-B). However, SAD erythrocyte MPs induced a 30% reduction in blood flow velocity in SAD renal arteries (Figure 3A; $P < .05$ vs none). Systolic blood flow velocity was unchanged after MP injection, but diastolic and mean blood flow velocities were dramatically decreased, as shown in representative echo-Doppler waveforms (Figure 3B). None of the MPs injections affected cardiac output (Figure 3C) or heart rate significantly (Figure 3D). Interestingly, SAD erythrocyte MPs had moderate effects in wild-type recipient mice, and so had wild-type erythrocyte MPs administered to SAD mice with 15% to 20% reductions in blood flow velocities ($P < .05$ vs controls; Figure 3). Moreover, Masson trichrome analysis of renal histology revealed cell aggregates and vascular congestion in the medulla of SAD kidneys but not in wild-type kidneys (Figure 3E). These aggregates consisted mainly of erythrocytes, with very few nucleated cells (supplemental Figures 2-3).

At 300×10^3 MPs/mouse, SAD RBC MPs induced a 35% reduction in mean blood flow velocity in SAD renal arteries (Figure 3A; $P < .05$ vs none). Diastolic and mean blood flow velocities were dramatically decreased (Figure 3B) without significant change in cardiac output (Figure 3C), heart rate (Figure 3D), or blood pressure (supplemental Figure 4).

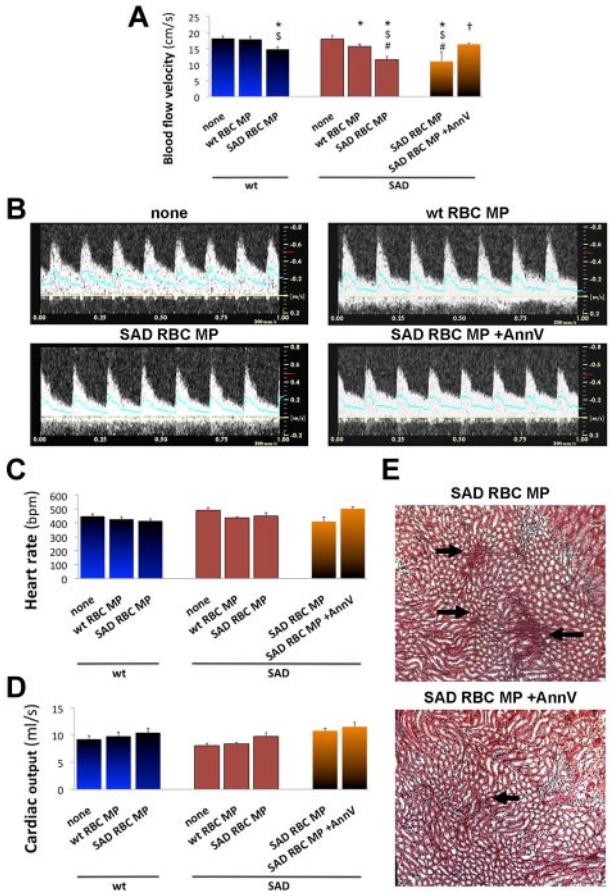

Figure 3. RBC MPs trigger vaso-occlusive crises in SAD mice. We injected 5×10^3 (blue and brown) or 300×10^3 RBC MPs/mouse (yellow) intravenously to wild-type (WT) or SAD transgenic mice. We monitored vaso-occlusion in kidneys by echo-Doppler recording of hemodynamic parameters in vivo. (A) We determined mean blood flow velocity (cm/s) in the right renal artery. Measures were acquired before (none), or after injection of WT or SAD RBC MPs (*$P < .05$ vs control, none; #$P < .05$ vs SAD RBC MPs [5×10^3 MPs/mouse]; \$$P < .05$ vs WT RBC MPs; †$P < .05$ vs SAD RBC MPs [300×10^3 MPs/mouse]). In some experiments, SAD RBC MPs were pre-incubated with annexin-V before injection. (B) Representative echo-Doppler waveforms in the renal artery of SAD mice before and after injection of WT or SAD RBC MPs, with or without preincubation with annexin-V. We also determined the heart rate (C; beats per minutes) and calculated the cardiac output (D; mL/min) from recording in the pulmonary artery. (E) Histologic analysis of SAD kidneys 5 minutes after injection of SAD RBC MPs, alone or pre-incubated with annexin-V, by Masson trichrome staining. Green arrows show areas of vascular congestion and erythrocyte deposits.

In other experiments, purified SAD RBC MPs were pre-incubated with annexin-V to saturate surface PS. Annexin-V–saturated MPs injected into SAD mice (300×10^3 MPs/mouse) failed to modify renal blood flow velocity or histology (Figure 3; $P < .05$ vs SAD RBC MPs; $P > .5$ vs controls).

Erythrocyte MPs activate endothelial cells and compromise vasodilation

We investigated the impact of erythrocyte MPs on murine endothelial monolayers cultured in 0.2 μm-filtered medium supplemented with wild-type or SAD RBC MPs. We analyzed ROS production, RBC adhesion, and endothelial apoptosis. Fresh wild-type RBC MPs (25 MPs/μL) stimulated significant but modest endothelial ROS production over basal levels, detected by H_2DFF-DA fluorescence after 2 hours (+10%; $P < .05$; Figure 4A). In contrast, SAD RBC MPs doubled endothelial ROS generation ($P < .05$ vs wild-type MPs). This was entirely inhibited when the MPs PS was previously saturated with recombinant annexin-V (1 μg/mL for 1 hour), and prevented when endothelial NADPH oxidase was inhibited with 10μM DPI or 100μM apocynin for 30 minutes, or when endothelial PKC activity was inhibited with 1μM Ro-31-8220 or 1μM Gö-6976 ($P < .05$ vs MPs alone).

Healthy wild-type erythrocytes did not adhere to confluent endothelial monolayers (less than 5 cells/field; Figure 4B-C). SAD erythrocytes adhered to endothelium twice more than wild-type cells, with or without pretreatment ($P < .05$). Priming endothelium with wild-type erythrocyte MPs (25 MPs/μL for 2 hours) had limited effects on wild-type and SAD erythrocyte adhesion (+20%; $P < .05$; Figure 4B). However, SAD RBC adhesion was increased

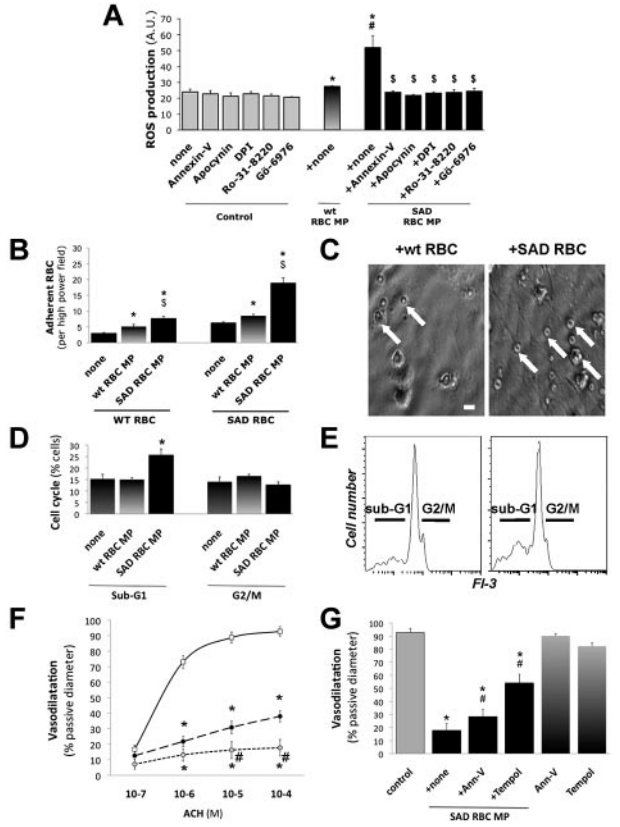

Figure 4. RBC MPs mediate vascular endothelial damage in vitro and ex vivo. (A) MPs shed by wild-type (WT) and SAD RBC treated with 4N1-1 were purified and incubated on confluent murine SVEC-40 endothelial monolayers (25 MPs/μL). The cells were pretreated with inhibitors of NADPH oxydase (apocynin, 100μM; DPI, 10μM) or protein-C kinase (Gö-6976, 1μM; Ro-31-8220, 1μM) for 30 minutes. Alternatively, RBC MPs were pre-incubated with annexin-V (10 μg/mL) for 30 minutes. Fluorescent H_2DFF-DA was added after 30 minutes and ROS production measured after 90 minutes. (*$P < .05$ vs WT control, none; #$P < .05$ vs WT MPs; \$$P < .05$ vs SAD MPs+none). (B) Endothelial monolayers were exposed to RBC MPs for 30 minutes and washed off. RBCs were then left to adhere for 30 minutes. Nonadherent RBCs were eliminated and adherent RBCs counted (*$P < .05$ vs no MPs; \$$P < .05$ vs WT MPs). (C) Representative micrographs of SAD RBC adhered to endothelium pre-treated with WT and SAD MPs (60×, bar is 5 μm). (D) Endothelial cells were treated with WT or SAD RBC MPs for 36 hours. Total DNA content was analyzed by FACS after propidium iodide coloration. Cells undergoing apoptosis (Sub-G_1 phase) or proliferation (G_2/M) were quantified. (E) Representative DNA profiles of endothelial cells incubated with WT or SAD RBC MPs for 16 hours (*$P < .05$ vs control, none). (F-G) Mesenteric resistances arteries were perfused with PSS alone, or supplemented with WT or SAD RBC MPs (200 MPs/μL) at 75 mmHg pressure and 20 μL/s flow. (F) Vasodilation in response to increasing ACH doses (10^{-4} to 10^{-7}M) was quantified and expressed as percentage of passive diameter (*$P < .05$ vs control [solid line]; #$P < .05$ vs WT RBC MPs [dashes]). (G) Vessels were pretreated with ROS inhibitor Tempol (10μM; 30 minutes), or SAD MPs were saturated with annexin-V (1 μg/mL; 1 hour) before perfusion (*$P < .05$ vs control; #$P < .05$ vs SAD RBC MPs alone, +none).

approximately 3-fold on endothelium primed with SAD erythrocyte MPs ($P < .05$ vs control).

In other experiments (Figure 4D-E), we primed endothelial monolayers with erythrocyte MPs for 36 hours in 0.05% NCS only. Wild-type MPs had did not modulate cell cycling, neither proliferation (G_2/M phase) nor apoptosis (sub-G_1 fraction). However, SAD MPs doubled endothelial apoptosis versus wild-type MPs ($P < .05$).

In other experiments, mesenteric resistance arteries were perfused with PSS in a pressure myograph. Initial diameter was measured as control. Arteries were preconstricted with phenylephrine and we assessed endothelium-dependent vasodilation in response to increasing doses of ACH (10^{-7}M to 10^{-4}M). The arteries were washed and preconstricted again. PSS, SAD, or wild-type erythrocyte MPs were then perfused. Vasodilation was measured again in response to the increasing ACH concentrations (Figure 4F). Perfusing erythrocyte MPs strongly reduced the sensitivity of resistance arteries to ACH-mediated vasodilation. SAD erythrocyte MPs blocked vasodilation even further than wild-type erythrocyte MPs ($P < .05$), resulting in near complete abrogation of vasodilation.

Alternatively, vasodilation was evaluated in response to saturating concentrations of NO donor SNP. PE and ACH treatments had no impact on subsequent SNP-induced vasodilation, consistent with intact smooth muscle (90% ± 3% of maximal vessel diameter). In contrast, wild-type and SAD erythrocyte MPs reduced SNP vasodilation down to 69% ± 5% and 59% ± 6%, respectively ($P < .05$ vs control; supplemental Figure 5).

Saturating MPs PS with recombinant annexin-V (1 μg/mL; 1 hour), or treating the vessels with the superoxide dismutase mimetic Tempol (10μM; 30 minutes) reduced the deleterious effects of SAD MPs (−20% and −50% of their respective effects; $P < .05$ vs MPs alone; Figure 4G). Tempol alone had little effects on vasodilation (−5% vessel diameter, $P < .05$ vs control).

Discussion

TSP1 raises circulating PS$^+$ MPs and renal vaso-occlusion in SAD mice

We addressed the concept that TSP1 favors vascular occlusions in SCD. We injected TSP1 intravenously at 1 mg/Kg to mimic a 5-fold increase in plasma, representing maximal platelet degranulation. In healthy wild-type mice, Hoylaerts and colleagues reported basal plasma TSP1 levels of 1.8 μg/mL.[15] Moreover, plasma TSP1 increases sharply during human VOCs (up to 5-fold).[12] In transgenic SAD mice, raising plasma TSP1 induced a dramatic 35% reduction in the diastolic and mean blood flow velocities within minutes, without concurrent impact on systemic hemodynamic parameters. The drop in kidney perfusion is thus consistent with increased renal vascular resistance and vascular occlusions, as confirmed by the histologic assessment of red blood cells aggregates and vascular congestion. TSP1 had little impact on kidney perfusion or systemic hemodynamic parameters in wild-type mice. The deleterious effects of TSP1 were only revealed in transgenic SAD mice, in territories susceptible to vaso-occlusions.[29,30] Within 5 minutes of TSP1 injection, SAD PFP contained 3 times as many PS$^+$ MPs. SAD mice at rest also contained at least twice as many circulating MPs as wild-type mice. We found the proportion of Ter119+ MPs (15%-30%) in SAD mice consistent with an over-representation of erythrocyte MPs versus wild-type mice (less than 5%), as observed in human SCD. The increase in plasma MPs coincided with vascular occlusions in SAD kidneys. The CD47 agonist 4N1-1 also induced a 3-fold rise in circulating PS$^+$ MPs, and the majority of wild-type and SAD erythrocytes expressed cell-surface CD47. The data agree with a release of MPs in response to CD47 activation.

TSP1 triggers discocyte conversion into echinocyte in connection with MP shedding

Because human VOCs are associated with drastic erythrocyte remodeling, we wondered whether TSP1 triggered direct erythrocyte modifications as observed during VOCs in humans. The microscopic analysis of mouse erythrocytes showed that adding TSP1 to wild-type discocytes induced crenation within 2 minutes and produced 10% of deformed cells (nondiscocyte). Scanning electron microscopy showed that the deformed erythrocytes were covered in cone-shaped membrane spicules and their phenotype was consistent with previously described echinocytes.[1,3] This pattern of short spicules corresponded to that predicted by surface tension analyses in WT erythrocytes,[37,38] and to that reported in response to Ca^{2+} ionophore A23187[39] or ATP depletion.[3] TSP1-CD47 signaling was previously reported to include rapid cytosolic Ca^{2+} mobilization,[40] cytoskeletal remodeling[41,42] and membrane PS externalization in various cell types.[42-44] CD47 may thus mediate similar effects in erythrocytes to enable those phenotypic changes.

At rest, SAD erythrocytes displayed only 5% of elongated sickle cells. Echinocytes with some degree of crenation or presenting spicules accounted for up to one-third of all erythrocytes. Adding TSP1 further increased SAD echinocytes with abnormal shapes and unpredictable numbers of longer and thinner spicules. Abnormal echinocytes exist in SCD patient blood at steady-state, and they are particularly present during VOCs.[2]

The CD47 agonist 4N1-1 induced echinocytes, such as TSP1, whereas control peptides did not. 4N1-1 also increased the numbers of thin, long, and apparently fragile spicules in SAD cell, whereas spicule numbers and dimensions remained homogenous in wild-type echinocytes.

TSP1 and 4N1-1 also triggered intense MP shedding in SAD and wild-type cells. MP shedding was concurrent to discocyte conversion into echinocytes, PS externalization, and spicule formation. This is consistent with reports on the correlation of PS externalization with spicule formation[39,45] and the suggested role of spicules in erythrocyte vesiculation.[1,46] The induction of erythrocyte vesiculation by TSP1 was significant at the near-physiologic levels of 10 μg/mL.

SAD and wild-type erythrocytes all respond to TSP1-CD47 signals by forming spicules, but SAD responses exceeded that of wild-type erythrocytes, and SAD cells were more prone to vesiculate. Some intrinsic characteristics of SAD erythrocytes, which we can relate to mutated hemoglobin, affect the phenotype to produce these abnormally thin and elongated spicules, and increase vesiculation. MP shedding may thus be associated with the relative fragility of echinocyte spicules. In contrast, TSP1 and 4N1-1 did not affect the proportion of elongated sickle cells, which bear very few spicules. We assume that sickle cell formation is ruled by different mechanisms or kinetics.

One difference between TSP1 and 4N1-1 is that shear rate was necessary to unmask the effects of TSP1, whereas 4N1-1 remained active at rest. Shear rate may synergize with the TSP1 carboxyterminus to facilitate CD47 activation. Indeed, CD47 has already been proposed as a mechanosensor, and CD47 signaling is strongly

enhanced by shear in SCD erythrocytes.[25] Furthermore, the amplitude of MP shedding was much enhanced when erythrocytes were placed in RPMI-1640 medium instead of PVP. It is possible that decreased viscosity may sensitize erythrocytes to vesiculation, whereas PVP may preserve erythrocyte membranes. Dedicated molecular studies will be needed to determine precisely how shear rate and viscosity influence CD47 activation by TSP1 and MPs shedding. Next, we aimed to establish the functional significance of these erythrocyte MPs.

SAD erythrocyte MPs induce renal vaso-occlusion

We investigated the impact of erythrocyte MPs on vascular occlusions in SAD mice. MPs derived from erythrocytes treated with 4N1-1 peptide in vitro were concentrated and purified. MPs were administered intravenously at low dose (8×10^3 MPs/mouse) to induce a 20% increase relative to circulating Ter119+ erythrocyte MPs compared with wild-type mouse levels, or at high dose (300×10^3 MPs/mouse) to increase total circulating PS+ MP levels by one-third compared with wild-type mice. At low dose, wild-type erythrocyte MPs had no significant impact on blood flow velocity in wild-type renal arteries (Figure 3A-B), nor on cardiac parameters nor on blood pressure. However, SAD erythrocyte MPs induced a 35% reduction in perfusion and vascular congestion in the medulla of SAD kidneys (supplemental Figure 2), without changing cardiac parameters or blood pressure. Similar results were obtained regarding brain perfusion, with a reduction of 20% after SAD erythrocyte MP injection in SAD mice. Raising SAD erythrocyte MPs increased local vascular resistance and produced severe vaso-occlusions in our mouse model.

The effects of SAD erythrocyte MPs were mainly similar in amplitude at low and high dose, underlying the pathophysiologic significance of moderate increases in circulating MP levels. However, the duration of vaso-occlusive events appeared much longer (more than 30 minutes) with high doses versus low doses (return to normal velocities within 20 minutes), although this was not precisely documented.

Models of vaso-occlusions versus human vaso-occlusive crises

We and others exposed transgenic SAD mice to hypoxia-reoxygenation to try and reproduce some of the clinical manifestations of SCD. SAD mice were found to recapitulate multiple features of human vaso-occlusive crises,[4] including erythrocyte dehydration, oxidative stress, tissue damage, and death.[30] SAD mice are thought to be less anemic than human patients, but their erythrocytes do mimic their human SCD counterparts. Hence, SAD mice have been widely used in pathophysiology reports. Other mouse models are devoid of murine hemoglobin and express human α, γ, or βS globins only.[47,48] These models display increased anemia, enhanced vascular damage, and shorter life expectancy compared with SAD mice. Their increased break down is expected to generate more erythrocyte-derived MPs and these mice may be well suited for experiments demonstrating that erythrocyte MPs are linked to vascular lesions. Indeed, knock-in homozygous HbS and Berkeley mice are prone to unpredictable spontaneous vaso-occlusive events.

It is critical to distinguish microvascular occlusive events in mice from the bundle of symptoms that characterize human VOCs (ie, hemolysis, ischemic tissue injury, and intense pain). Here, injecting MPs created an acute rise in plasma MPs, but circulating MPs are thought to be rapidly cleared by the spleen, liver, and lungs.[49] Our model is more appropriate to demonstrate the vascular impact of MPs than it is to represent chronic exposure. The drop in renal perfusion induced with MPs injection was rapid but temporary, and lasted approximately 20 to 30 minutes. SAD erythrocyte MPs injected to SAD mice did sometimes trigger prostration and rough hair coat, which paralleled the drop in renal perfusion. This sign of pain might be compared with the acute pain felt by SCD patients during VOCs, although the comparison is difficult to uphold because we did not observe widespread oxidative injury in the kidneys or creatinine hyperfiltration (supplemental Figures 3-4) within 2 hours of the injection.

SAD erythrocyte MPs mediate endothelial injury and vascular dysfunction

We investigated the impact of erythrocyte MPs on cultured endothelium and isolated microvessels. We found that SAD erythrocyte MPs compromised vasodilation in perfused microvessels, favored SAD erythrocyte adhesion, and caused endothelial injury in the long-term. These effects are thought to be critical to vaso-occlusions in mouse and human SCD. In all cases, wild-type erythrocyte MPs had much reduced effects versus SAD at similar concentrations. Erythrocyte MPs will be particularly deleterious in SAD mice where they are present in greater numbers. Endothelial activation by erythrocyte MPs may thus represent a critical step to trigger erythrocyte adhesion, block vasodilation, and favor vaso-occlusion.

Erythrocyte MPs may target vascular endothelial cells and compromise primarily endothelial-dependent function. However, we also found that exposure of microvessels to erythrocyte MPs reduced SNP-induced vasodilation (−15% and −25% for wild-type and SAD MPs, respectively; $P < .05$), consistent with some additional injury to the smooth muscle (supplemental Figure 4D).

Fresh wild-type erythrocyte MPs only stimulated modest endothelial ROS production over basal levels, but SAD erythrocyte MPs more than doubled ROS production at similar concentrations. These superior effects on endothelial ROS production paralleled those on erythrocyte adhesion, apoptosis, and vasodilation in vitro, as well as vaso-occlusion in vivo. In perfused microvessels, the deleterious effects of SAD erythrocyte MPs were blocked and the ACH-mediated vasodilation was preserved by the superoxide dismutase mimetic Tempol. The effects of SAD MPs were not entirely blocked by Tempol. This implies that other mechanisms of erythrocyte MPs toxicity may be at play, even if endothelial ROS production seems particularly targeted by SAD erythrocyte MPs. In vitro, endothelial ROS generation was prevented with specific NADPH oxidase and PKC inhibitors, suggesting that erythrocyte MPs activate these enzymes to generate excess superoxide.

ROS generation induced by SAD erythrocyte MPs was entirely inhibited when PS was previously saturated with recombinant annexin-V. The deleterious effects of erythrocyte MPs were mediated by ROS in both isolated microvessels and cultured endothelium, in a manner partially dependent on PS. The saturation of PS with annexin-V at the surface of SAD erythrocyte MPs also abrogated their impact on kidney perfusion in vivo. This suggested that externalized PS is a key functional feature of circulating erythrocyte MPs that could mediate excess endothelial ROS production and vaso-occlusions in SCD. The inhibitory effects of recombinant annexin-V may open novel therapeutic possibilities to treat SCD patients.

Sickle cell disease is a vascular disease?

Interestingly, the reduction of kidney perfusion in vivo was maximal when erythrocyte MPs and recipient mice were all of SAD genotype. Moreover, maximal stimulation of erythrocyte adhesion to endothelial cells was obtained when erythrocyte MPs and adherent erythrocytes were of SAD genotype; This suggested a synergy between the MP populations and altered vascular function. Hence, SAD erythrocyte MPs may synergize with intrinsic SAD erythrocyte and vascular features to maximize adhesion, compromise vasodilation, and induce vaso-occlusions. It is also possible that endothelial activation by erythrocyte MPs triggers the secretion of endothelial vasoconstriction factors such as endothelin-1,[30] enhancing further vaso-occlusions.

Moreover, the mechanisms of cell activation by erythrocyte MPs seem to progress through PS pathways potentially recognized by multiple cell types. Although our results did not point toward a particularly high representation of leukocytes in our MP-induced vaso-occlusions in kidneys (supplemental Figure 3), it would be interesting to study the effects of MPs on inflammatory cells and more particularly on neutrophils, which may participate in vaso-occlusive events.

Summary

Increased plasma TSP1 stimulated the shedding of erythrocyte MPs in the bloodstream. These erythrocyte MPs are sufficient to induce vaso-occlusions in a mouse model of SCD, and enhance several processes thought to facilitate vaso-occlusions, namely impaired vasodilation, RBC adhesion, and endothelial damage. Our data place erythrocyte MPs in a key position to participate in the manifestations of SCD. Further experiments will be necessary to determine the importance of the TSP1 pathway in human SCD and the role of erythrocyte MPs in the development of painful VOCs and the vasculopathy associated with SCD in humans.

Acknowledgments

The authors thank Dr Arnaud Bonnefoy (Montreal Heart Institute, Canada) for expert advice with TSP1 biology, Isabel Le Disquet (Université Pierre et Marie Curie-Paris VI, France) for excellent assistance at the electron microscopy department, and Dr Ratiba Nih (Inserm U965, Paris, France) for help with animal studies.

This work was supported by the Agence Nationale pour la Recherche (ANR-Physio2007 P005432 to O.P.B.-B. and L.L.), the CNRS and Inserm. S.C. benefited from Ministere de l'Education Nationale de la Recherche et de Technologie doctoral fellowships of the French government and from a grant from the Fondation pour la Recherche Médicale (FDT 2011-0922471). J.A.D.M. was funded by the Franco-Brasilian exchange program CAPES-COFECUB (629/09 to O.P.B.-B.).

Authorship

Contribution: S.M.C. conceived and designed the study, collected and/or assembled data, analyzed and interpreted data, and wrote the paper; B.G., L.G., D.C., J.A.D.M., and J.-M.R. collected and/or assembled data; P.B. and L.L. collected and/or assembled data and analyzed and interpreted data; A.T. obtained financial support; C.M.B. and P.-L.T. conceived and designed the study and obtained financial support; and O.P.B.-B. conceived and designed the study, obtained financial support, analyzed and interpreted data, and wrote and approved the final paper.

Conflict-of-interest disclosure: The authors declare no competing financial interests.

Correspondence: Olivier P. Blanc-Brude, Paris Center for Cardiovascular Research, Inserm U970, Hôpital Européen Georges Pompidou, 56 rue Leblanc, F-75010 Paris, France; e-mail: olivier.blanc-brude@inserm.fr.

References

1. Allan D, Limbrick AR, Thomas P, Westerman MP. Release of spectrin-free spicules on reoxygenation of sickled erythrocytes. *Nature.* 1982; 295(5850):612-613.
2. Warth JA, Rucknagel DL. Density ultracentrifugation of sickle cells during and after pain crisis: increased dense echinocytes in crisis. *Blood.* 1984; 64(2):507-515.
3. Chabanel A, Reinhart W, Chien S. Increased resistance to membrane deformation of shape-transformed human red blood cells. *Blood.* 1987; 69(3):739-743.
4. Nath KA, Katusic ZS. Vasculature and kidney complications in sickle cell disease. *J Am Soc Nephrol.* 2012;23(5):781-784.
5. Wun T, Paglieroni T, Tablin F, Welborn J, Nelson K, Cheung A. Platelet activation and platelet-erythrocyte aggregates in patients with sickle cell anemia. *J Lab Clin Med.* 1997;129(5):507-516.
6. Setty BN, Kulkarni S, Rao AK, Stuart MJ. Fetal hemoglobin in sickle cell disease: relationship to erythrocyte phosphatidylserine exposure and coagulation activation. *Blood.* 2000;96(3):1119-1124.
7. Westerman M, Pizzey A, Hirschman J, et al. Microvesicles in haemoglobinopathies offer insights into mechanisms of hypercoagulability, haemolysis and the effects of therapy. *Br J Haematol.* 2008;142(1):126-135.
8. Mahfoudhi E, Lecluse Y, Driss F, Abbes S, Flaujac C, Garcon L. Red cells exchanges in sickle cells disease lead to a selective reduction of erythrocytes-derived blood microparticles. *Br J Haematol.* 2012; 156(4):545-547.
9. Shet AS, Aras O, Gupta K, et al. Sickle blood contains tissue factor-positive microparticles derived from endothelial cells and monocytes. *Blood.* 2003;102(7):2678-2683.
10. van Tits LJ, van Heerde WL, Landburg PP, et al. Plasma annexin A5 and microparticle phosphatidylserine levels are elevated in sickle cell disease and increase further during painful crisis. *Biochem Biophys Res Commun.* 2009;390(1): 161-164.
11. van Beers EJ, Schaap MC, Berckmans RJ, et al. Circulating erythrocyte-derived microparticles are associated with coagulation activation in sickle cell disease. *Haematologica.* 2009;94(11):1513-1519.
12. Browne PV, Mosher DF, Steinberg MH, Hebbel RP. Disturbance of plasma and platelet thrombospondin levels in sickle cell disease. *Am J Hematol.* 1996; 51(4):296-301.
13. Beurling-Harbury C, Schade SG. Platelet activation during pain crisis in sickle cell anemia patients. *Am J Hematol.* 1989;31(4):237-241.
14. Bonnefoy A, Daenens K, Feys HB, et al. Thrombospondin-1 controls vascular platelet recruitment and thrombus adherence in mice by protecting (sub)endothelial VWF from cleavage by ADAMTS13. *Blood.* 2006;107(3):955-964.
15. Bonnefoy A, Moura R, Hoylaerts MF. The evolving role of thrombospondin-1 in hemostasis and vascular biology. *Cell Mol Life Sci.* 2008;65(5): 713-727.
16. McLaughlin JN, Mazzoni MR, Cleator JH, et al. Thrombin modulates the expression of a set of genes including thrombospondin-1 in human microvascular endothelial cells. *J Biol Chem.* 2005; 280(23):22172-22180.
17. Phelan MW, Forman LW, Perrine SP, Faller DV. Hypoxia increases thrombospondin-1 transcript and protein in cultured endothelial cells. *J Lab Clin Med.* 1998;132(6):519-529.
18. Frangogiannis NG, Ren G, Dewald O, et al. Critical role of endogenous thrombospondin-1 in preventing expansion of healing myocardial infarcts. *Circulation.* 2005;111(22):2935-2942.
19. Sajid M, Hu Z, Guo H, Li H, Stouffer GA. Vascular expression of integrin-associated protein and thrombospondin increase after mechanical injury. *J Investig Med.* 2001;49(5):398-406.
20. McPherson J, Sage H, Bornstein P. Isolation and characterization of a glycoprotein secreted by aortic endothelial cells in culture. Apparent identity with platelet thrombospondin. *J Biol Chem.* 1981;256(21):11330-11336.
21. Freyberg MA, Kaiser D, Graf R, Buttenbender J, Friedl P. Proatherogenic flow conditions initiate endothelial apoptosis via thrombospondin-1 and the integrin-associated protein. *Biochem Biophys Res Commun.* 2001;286(1):141-149.
22. Moura R, Tjwa M, Vandervoort P, Cludts K, Hoylaerts MF. Thrombospondin-1 activates medial smooth muscle cells and triggers neointima formation upon mouse carotid artery ligation. *Arterioscler Thromb Vasc Biol.* 2007;27(10):2163-2169.
23. Brittain HA, Eckman JR, Swerlick RA, Howard RJ,

Wick TM. Thrombospondin from activated platelets promotes sickle erythrocyte adherence to human microvascular endothelium under physiologic flow: a potential role for platelet activation in sickle cell vaso-occlusion. *Blood.* 1993;81(8):2137-2143.

24. Brittain JE, Mlinar KJ, Anderson CS, Orringer EP, Parise LV. Integrin-associated protein is an adhesion receptor on sickle red blood cells for immobilized thrombospondin. *Blood.* 2001;97(7):2159-2164.
25. Brittain JE, Mlinar KJ, Anderson CS, Orringer EP, Parise LV. Activation of sickle red blood cell adhesion via integrin-associated protein/CD47-induced signal transduction. *J Clin Invest.* 2001; 107(12):1555-1562.
26. Brittain JE, Han J, Ataga KI, Orringer EP, Parise LV. Mechanism of CD47-induced alpha4beta1 integrin activation and adhesion in sickle reticulocytes. *J Biol Chem.* 2004;279(41):42393-42402.
27. Trudel M, Saadane N, Garel MC, et al. Towards a transgenic mouse model of sickle cell disease: hemoglobin SAD. *EMBO J.* 1991;10(11):3157-3165.
28. Kosfeld MD, Frazier WA. Identification of a new cell adhesion motif in two homologous peptides from the COOH-terminal cell binding domain of human thrombospondin. *J Biol Chem.* 1993; 268(12):8808-8814.
29. Bonnin P, Sabaa N, Flamant M, Debbabi H, Tharaux PL. Ultrasound imaging of renal vaso-occlusive events in transgenic sickle mice exposed to hypoxic stress. *Ultrasound Med Biol.* 2008;34(7):1076-1084.
30. Sabaa N, de Franceschi L, Bonnin P, et al. Endothelin receptor antagonism prevents hypoxia-induced mortality and morbidity in a mouse model of sickle-cell disease. *J Clin Invest.* 2008;118(5): 1924-1933.
31. Leroyer AS, Ebrahimian TG, Cochain C, et al. Microparticles from ischemic muscle promotes postnatal vasculogenesis. *Circulation.* 2009; 119(21):2808-2817.
32. Loufrani L, Levy BI, Henrion D. Defect in microvascular adaptation to chronic changes in blood flow in mice lacking the gene encoding for dystrophin. *Circ Res.* 2002;91(12):1183-1189.
33. Gao AG, Lindberg FP, Finn MB, Blystone SD, Brown EJ, Frazier WA. Integrin-associated protein is a receptor for the C-terminal domain of thrombospondin. *J Biol Chem.* 1996;271(1):21-24.
34. McDonald JF, Dimitry JM, Frazier WA. An amyloid-like C-terminal domain of thrombospondin-1 displays CD47 agonist activity requiring both VVM motifs. *Biochemistry.* 2003;42(33):10001-10011.
35. Isenberg JS, Ridnour LA, Dimitry J, Frazier WA, Wink DA, Roberts DD. CD47 is necessary for inhibition of nitric oxide-stimulated vascular cell responses by thrombospondin-1. *J Biol Chem.* 2006;281(36):26069-26080.
36. Floquet N, Dedieu S, Martiny L, Dauchez M, Perahia D. Human thrombospondin's (TSP-1) C-terminal domain opens to interact with the CD-47 receptor: a molecular modeling study. *Arch Biochem Biophys.* 2008;478(1):103-109.
37. Lim HWG, Wortis M, Mukhopadhyay R. Stomatocyte-discocyte-echinocyte sequence of the human red blood cell: evidence for the bilayer-couple hypothesis from membrane mechanics. *Proc Natl Acad Sci U S A.* 2002;99(26): 16766-16769.
38. Mukhopadhyay R, Lim HWG, Wortis M. Echinocyte shapes: bending, stretching, and shear determine spicule shape and spacing. *Biophys J.* 2002;82(4):1756-1772.
39. Bratosin D, Estaquier J, Petit F, et al. Programmed cell death in mature erythrocytes: a model for investigating death effector pathways operating in the absence of mitochondria. *Cell Death Differ.* 2001;8(12):1143-1156.
40. Schwartz MA, Brown EJ, Fazeli B. A 50-kDa integrin-associated protein is required for integrin-regulated calcium entry in endothelial cells. *J Biol Chem.* 1993;268(27):19931-19934.
41. Tsao PW, Mousa SA. Thrombospondin mediates calcium mobilization in fibroblasts via its Arg-Gly-Asp and carboxyl-terminal domains. *J Biol Chem.* 1995;270(40):23747-23753.
42. Mateo V, Brown EJ, Biron G, et al. Mechanisms of CD47-induced caspase-independent cell death in normal and leukemic cells: link between phosphatidylserine exposure and cytoskeleton organization. *Blood.* 2002;100(8):2882-2890.
43. Roué G, Bitton N, Yuste VJ, et al. Mitochondrial dysfunction in CD47-mediated caspase-independent cell death: ROS production in the absence of cytochrome c and AIF release. *Biochimie.* 2003;85(8):741-746.
44. Head DJ, Lee ZE, Swallah MM, Avent ND. Ligation of CD47 mediates phosphatidylserine expression on erythrocytes and a concomitant loss of viability in vitro. *Br J Haematol.* 2005;130(5): 788-790.
45. Sakthivel R, Farooq SM, Kalaiselvi P, Varalakshmi P. Investigation on the early events of apoptosis in senescent erythrocytes with special emphasis on intracellular free calcium and loss of phospholipid asymmetry in chronic renal failure. *Clin Chim Acta.* 2007; 382(1-2):1-7.
46. Iglic A, Veranic P, Jezernik K, et al. Spherocyte shape transformation and release of tubular nanovesicles in human erythrocytes. *Bioelectrochemistry.* 2004;62(2):159-161.
47. Pászty C, Brion CM, Manci E, et al. Transgenic knockout mice with exclusively human sickle hemoglobin and sickle cell disease. *Science.* 1997; 278(5339):876-878.
48. Wu LC, Sun CW, Ryan TM, Pawlik KM, Ren J, Townes TM. Correction of sickle cell disease by homologous recombination in embryonic stem cells. *Blood.* 2006;108(4):1183-1188.
49. Willekens FL, Werre JM, Kruijt JK, et al. Liver Kupffer cells rapidly remove red blood cell-derived vesicles from the circulation by scavenger receptors. *Blood.* 2005;105(5):2141-2145.